53. ASSIMILATION OF SMOS SOIL MOISTURE RETRIEVALS IN THE LAND INFORMATION SYSTEM

Clay B. Blankenship, USRA, Huntsville, Alabama
Bradley T. Zavodsky, NASA-MSFC, Huntsville, Alabama
Jonathan L. Case, ENSCO, Inc., Huntsville, Alabama

1 BACKGROUND

1.1 Overview

Soil moisture is a crucial variable for weather prediction because of its influence on evaporation, especially during warm-season months. It is also important for drought and flood monitoring prediction, and for public health applications. The NASA Short-term Prediction Research and Transition (SPoRT) Center has implemented a new module in the NASA Land Information System (LIS) to assimilate soil moisture retrievals from the European Space Agency's Soil Moisture and Ocean Salinity (SMOS) satellite. SMOS Level 2 retrievals from the Microwave Imaging Radiometer using Aperture Synthesis (MIRAS) instrument are assimilated into the Noah LSM within LIS via an Ensemble Kalman Filter. The retrievals have a target volumetric accuracy of 4% at a resolution of 35-50 km. Parallel runs with and without SMOS assimilation are performed with precipitation forcing from intentionally degraded observations, and then validated against a model run using the best available precipitation data, as well as against selected station observations. The goal is to demonstrate how SMOS data assimilation can improve modeled soil states in the absence of dense rain gauge and radar networks. Preliminary results are dominated by biases between the retrievals and the model background, but the assimilation successfully adds soil moisture in areas of strong signal (large precipitation).

1.2 The Land Information System

The NASA Land Information System (LIS, Kumar et al. 2006) is a modeling framework for running land surface models. To facilitate intercomparisons, users may select land surface models, forcing data sources, landcover and soil type data sources, and many other parameters. SPoRT uses LIS to produce real-time soil moisture products for situational awareness and local numerical weather prediction over CONUS, Mesoamerica, and East Africa (Case and White 2014; Case et al. 2014). Model output can be used to monitor and predict several phenomena including drought, fire, extreme heat, flooding, convective initiation, and water-borne diseases.

1.3 SMOS and SMAP

SPoRT is testing the assimilation of L-band (1.4 GHz) satellite soil moisture retrievals within LIS to improve modeled soil moisture and other output fields. Measurements at the L-band are more sensitive to surface soil moisture, and perform better in heavy vegetation, compared to previous (higher frequency) instruments. The work focuses on two satellite missions. The first is SMOS, launched in 2009, which carries the MIRAS radiometer. The second, upcoming mission is NASA's Soil Moisture Active/Passive (SMAP) mission (Entekhabi et al. 2010), scheduled for launch in late 2014, which will have a radiometer and also an L-band radar. The SMAP mission will produce products separately from both the radiometer (higher accuracy) and the radar (higher spatial resolution) as well as a combined product. Some parameters from these two missions are given in Table 1.

We are currently assimilating SMOS soil moisture retrievals. Experience from this work assimilation will facilitate the rapid implementation of SMAP data assimilation after SMAP is launched. We are members of the SMAP Early Adopters team (Brown et al. 2013) which will have early access to experimental data.

Name	SMOS Soil Moisture and Ocean Salinity	SMAP Soil Moisture Active/Passive	
Agency	ESA	NASA	
Launch	2009	Nov. 2014	
Orbit	Polar	Polar	
Sensor Type	Passive	Active	Passive
Frequency	1.4 GHz (L-band)	1.2 GHz	1.41 GHz
Resolution	35-50 km	>=1-3 km	36 km
Accuracy	4 cm^3/cm^3	6 cm^3/cm^3	4 cm^3/cm^3

Table 1. SMOS and SMAP characteristics.

2 SMOS ASSIMILATION IN LIS

2.1 Description

We assimilate AMSR-E soil moisture observations into the Noah 3.2 land surface model (Ek et al. 2003) within LIS (release 6.1) using an Ensemble Kalman Filter (EnKF). Kalman filtering is a data assimilation method that combines a forecast (background) with observations to generate an improved estimate of a model variable. A Kalman Filter calculates an optimal weighting between the background and the observation. The EnKF uses the spread of the ensemble to represent the forecast error covariance.

Taking advantage of the modular structure of LIS, we added a module to LIS to read SMOS Level 2 Soil Moisture User Data Product (SMUDP) files provided by ECMWF. Data are screened for radio frequency interference, frozen soil, snowcover, falling precipitation, heavy vegetation, and data quality flags.

2.2 Test Case

For a test case, we chose Tropical Cyclone Andrea in June 2013, shown in Figure 1. Before landfall, there was significant precipitation in Florida and Georgia associated with outlying rain bands. The EnKF runs

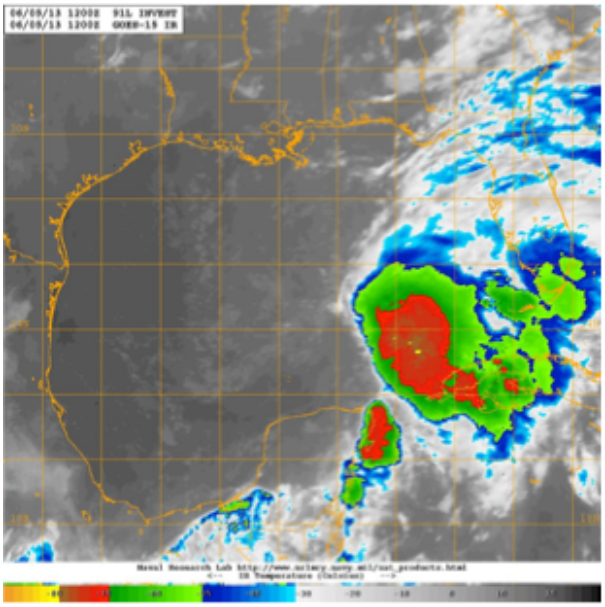

Figure 1. GOES IR image. Courtesy of Naval Research Laboratory, Monterey, CA.

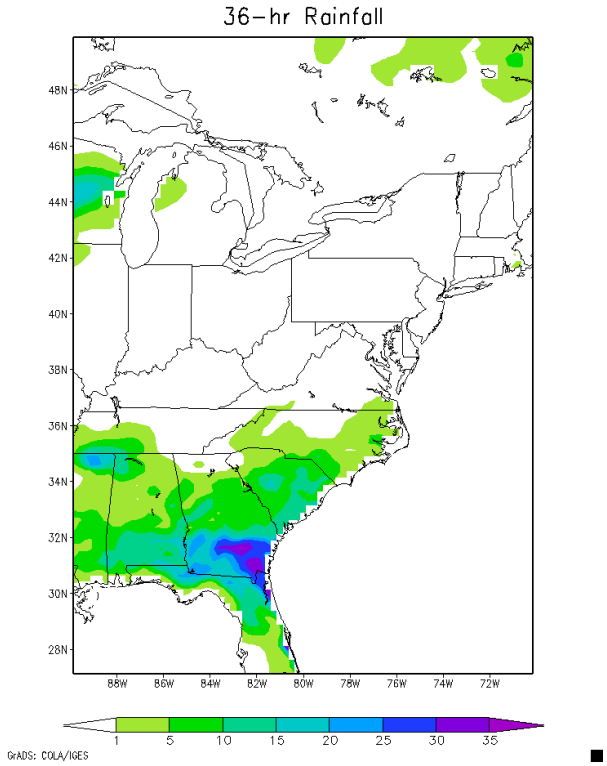

Figure 2. Thirty-six hour accumulated precipitation from GDAS forcing data

assimilated data at 0:00 and 12:00 UTC on 5 Jun 2013, with all observations occurring within 3 hours of the assimilation time or less. Results presented herein are from the 12:00 UTC assimilation step. The GDAS-analyzed accumulated precipitation for the 36 hours preceding the analysis time is shown in Figure 2, with a maximum occurring in southeastern Georgia.

2.3 Experiment Setup

Simulations of this event with and without data assimilation were run in LIS using the Noah 3.2 land surface model on an 80x92 grid over eastern North America at 25-km resolution. Each experiment run had an 8-month spinup prior to the assimilation. This is probably not sufficient to initialize the deep soil layers but it should be enough time to initialize the modeled soil moisture in the top few centimeters. This spinup period also serves to generate ensemble spread, a necessary component for the EnKF, from the perturbations. We used an ensemble with 16 members generated using perturbations of 3 forcing variables (incident longwave and shortwave radiation, and rainfall), 4 state variables (4 layers of soil moisture), and 1 observation variable (SMOS soil moisture). Perturbations were applied based on the AMSR-E test case values in the LIS distribution.

The Noah model was run with a 30-minute timestep and configured with the University of Maryland landcover database (Hansen et al. 2000) and the FAO soil database (FAO-UNESCO, 1977). It was driven with forcing data (temperature, humidity, winds, and incident radiation at the surface) from the Global Data Assimilation System (GDAS; Derber et al. 1991).

Experiment Name	Rain Forcing	Configuration	Purpose
Dry DA	0.5*GDAS	EnKF	Experiment 1
Dry Control	0.5*GDAS	Open Loop	Control 1
Wet DA	1.5*GDAS	EnKF	Experiment 2
Wet Control	1.5*GDAS	Open Loop	Control 2
"Truth" Run	GDAS	Single run	Validation

Table 2. Data assimilation experiment setup.

Validation of soil moisture assimilation can be challenging, particularly when using in situ measurements as ground truth, due to sampling issues and biases. Therefore we chose an artificial setup for an initial test of our methodology. We assimilated SMOS observations into two LIS simulations with intentionally degraded precipitation forcing (0.5 and 1.5 times the analysis values). We also performed two control (open loop) simulations, run in ensemble mode with perturbations but no assimilation. Setttings for these runs are summarized in Table 2. The results were compared to a run with no assimilation and the unaltered GDAS forcing. This is considered the "truth" run for verification purposes, but of course there are

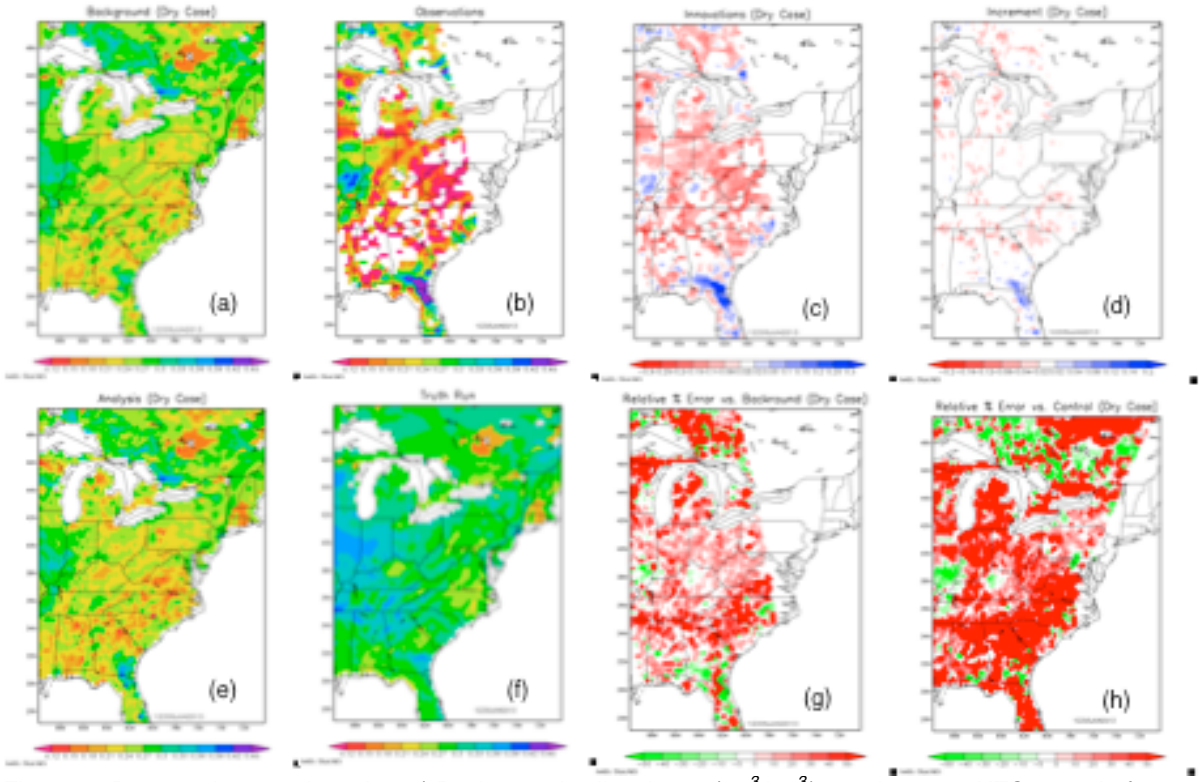

Figure 3. Dry case input and results. a) Background soil moisture (cm^3/cm^3) at 5 Jun 2013 UTC 12:00 before assimilation step. b) SMOS level 2 retrieved surface soil moisture (observations). c) Innovations (observations minus background). d) Model increment. e) Analysis after assimilation. f) "Truth" field with best forcing data. g) Error reduction (compared to background). h) Error reduction (compared to open loop run).

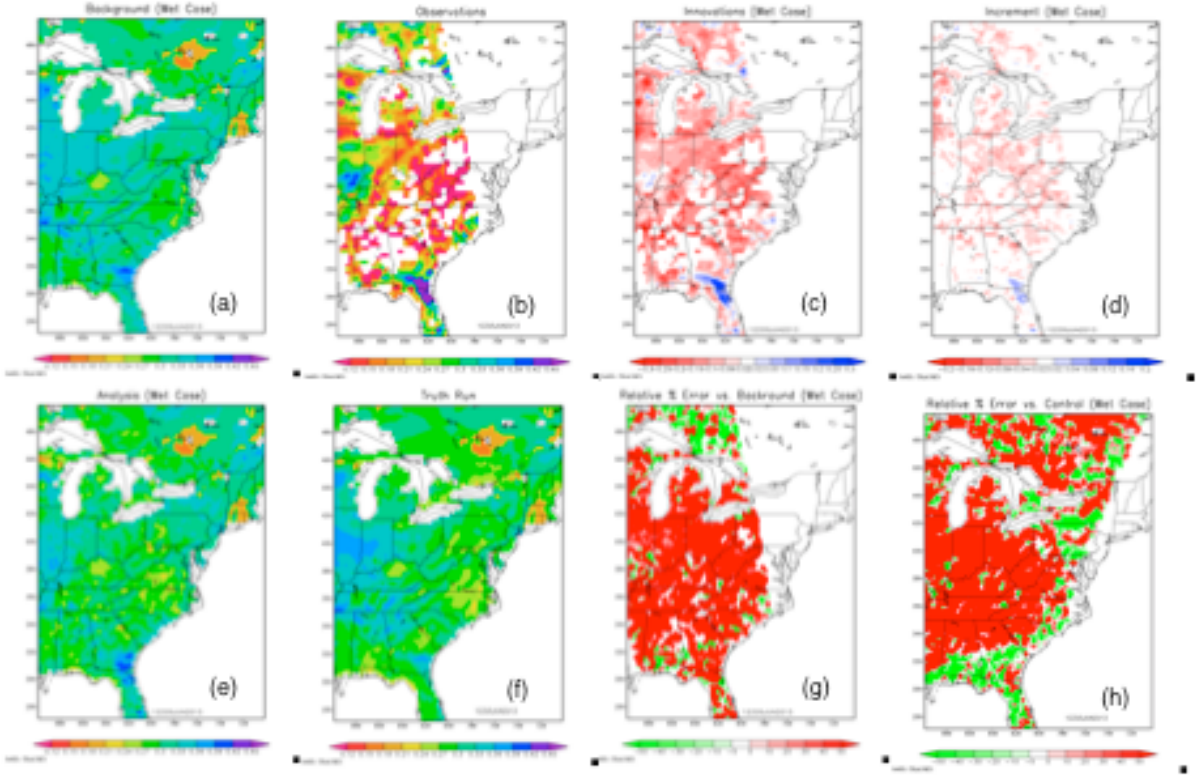

Figure 4. As figure 3, but for wet case.

errors in both the SMOS retrievals and the GDAS precipitation analyses so they should not be expected to agree completely. Nevertheless, we assume the errors in the "truth" run are small compared to the other runs with intentionally degraded forcing.

2.4 Results

Results from this experiment are shown in Figures 3 and 4 for the dry and wet simulations (+/- 50% GDAS precipitation forcing), respectively. Figures 3a and 4a show the initial (pre-assimilation) soil moisture content of the top (0-10 cm) model layer at 12:00 UTC on 5 Jun 2013. The values of the soil moisture retrievals that are assimilated (after quality control) are shown in Figures 3b and 4b. The next panels, Figures 3c and 4c, show the innovations, i.e. the observations, or retrievals, minus the model background. (Here we are making the assumption that the retrieved soil moisture, which is roughly from the top 2.5 cm, is equivalent to the 0-10 cm modeled soil moisture). Figures 3d and 4d depict the model increment that is applied by the data assimilation step. This is directly related to the innovation, but with a spatially-varying gain that depends on the ensemble spread at each point and the observation uncertainty. Figures 3e and 4e show the 0-10 cm soil moisture analyses (i.e. values after assimilation). Figures 3f and 4f (identical) show the "truth" value from the simulation with unmodified GDAS rain forcing.

The innovations (3c/4c) reveal a dry bias in the observations (relative to the model state), even for the "dry" model run, evident in the widespread negative values. In southeastern Georgia and northeastern Florida, the observed soil moisture values are high enough to overcome this bias. In the dry case we also see positive anomalies in southern Illinois.

The analysis increments (3d/4d) have a relatively weak magnitude compared to the innovations. The strength of the gain, as controlled by the magnitude of ensemble perturbations as well as the observation uncertainty, will be the subject of future research. The signs of the analysis agree with those of the innovation, as expected. The largest increments are in southeastern Georgia/northeastern Florida where the signal in the observations is strong enough to overcome the bias. This area shows increased moisture in the analyses (3e/4e), which is the desired outcome. In other areas, the changes are relatively small.

Panels g and h of Figures 3 and 4 show metrics calculated to perform a quantitative validation. Figures 3g and 4g show the error reduction due to a single data assimilation cycle, computed as

$$\left(\left|\frac{Analysis - Truth}{Background - Truth}\right| - 1\right) * 100$$

Areas shaded in green have a reduced absolute error (the analysis is closer to the "truth" than the background is). The bias dominates this analysis but where the signal is strongest, we do see an error reduction in the dry case.

Panels 3h and 4h are similar to 3g/4g, but the metric is calculated 12 hours later, at 0:00 UTC on 6 Jun 2013. This shows the impact of two assimilation cycles 12 hours apart. This metric still shows negative impact at most locations, due in part to the large model-observation bias, but the area with positive impact has increased. This suggests that perhaps that assimilating observations at multiple times may be having a positive impact.

The appearance of positive analysis increments where the precipitation signal was strongest is indicative that the assimilation cycle is running properly. However, it is clear that the model-observation biases are quite significant and need to be dealt with.

3 FUTURE IMPROVEMENTS

After speaking with several colleagues, we plan to apply a bias correction to the observations using a CDF-matching technique (Reichle and Koster 2004) with a separate curve matching applied for each broad land cover category (Blankenship and Crosson 2011). The assimilation will be tested in a cycling run over an extended period of time. We will perform validation in a less-vegetated region such as the Great Plains, where the soil moisture signal is strongest. This will enable us to use the Oklahoma Mesonet (Brock et al. 1995) for validation as well. Other improvements will include optimizing the ensemble perturbations to achieve a spread that is representative of the estimated model error, and determining the optimal observation uncertainty. We will test this methodology in a smaller, higher-resolution domain in order to assess its impact on various applications. Finally, we will implement this methodology with the simulated SMAP data that has been provided to SMAP Early Adopters, to prepare for the launch of SMAP.

4 ACKNOWLEDGEMENTS

This work is supported by Tsengdar Lee of the NASA Science Mission Directorate through SPoRT. We would also like to thank Susan Moran, Vanessa Escobar, and Molly Brown for including us as SMAP Early Adopters

5 REFERENCES

Blankenship, C. B. and W. Crosson, 2011: “Bias correction based on regime-dependent Cumulative Distribution Functions for soil moisture data assimilation in a Land Surface

Model", AMS Annual Meeting, Seattle, WA, Jan. 24-27, 2011.

Brock, Fred V., Kenneth C. Crawford, Ronald L. Elliott, Gerrit W. Cuperus, Steven J. Stadler, Howard L. Johnson, Michael D. Eilts, 1995: The Oklahoma Mesonet: A Technical Overview. *J. Atmos. Oceanic Technol.*, **12**, 5–19.

Brown, Molly E., Vanessa Escobar, Susan Moran, Dara Entekhabi, Peggy E. O'Neill, Eni G. Njoku, Brad Doorn, Jared K. Entin, 2013: NASA's Soil Moisture Active Passive (SMAP) Mission and Opportunities for Applications Users. *Bull. Amer. Meteor. Soc.*, **94**, 1125–1128.

Case, J. L., and K. D. White, 2014: Expansion of the real-time SPoRT-Land Information System for NOAA/National Weather Service situational awareness and local modeling applications. Preprints, *26th Conf. on Weather Analysis and Forecasting / 22nd Conf. on Numerical Weather Prediction,* Atlanta, GA, Amer. Meteor. Soc., P162. [Available online at https://ams.confex.com/ams/94Annual/webprogram/Paper235310.html]

Case, J. L., J. Mungai, V. Sakwa, E. Kabuchanga, B. T. Zavodsky, and A. S. Limaye, 2014: Toward improved land surface initialization in support of regional WRF forecasts at the Kenya Meteorological Service. Preprints, *26th Conf. on Weather Analysis and Forecasting / 22nd Conf. on Numerical Weather Prediction,* Atlanta, GA, Amer. Meteor. Soc., J9.4. [Available online at https://ams.confex.com/ams/94Annual/webprogram/Paper235263.html]

Derber, J. C., D. F. Parrish, and S. J. Lord, 1991: The new global operational analysis system at the National Meteorological Center. *Wea. Forecasting,* **6,** 538-547.

Ek, M. B., K. E. Mitchell, Y. Lin, E. Rogers, P. Grunmann, V. Koren, G. Gayno, and J. D. Tarpley, 2003: Implementation of Noah land surface model advances in the National Centers for Environmental Prediction operational mesoscale Eta model, *J. Geophys. Res.,* **108 (D22),** 8851.

Entekhabi, D. and Coauthors, 2010: "The Soil Moisture Active Passive (SMAP) mission," *Proc. IEEE*, **98 (5),** 704-716.

European Space Agency, 2002: *Mission Objectives and Scientific Requirements of the Soil Moisture and Ocean Salinity (SMOS) Mission,* Version 5. http://esamultimedia.esa.int/docs/SMOS_MRD_V5.pdf

FAO-UNESCO, 1977. Soil Map of the World, Africa. Puhl. FAO-UNESCO, Paris, 299 pp.

Hansen, M.C., R.S. DeFries, J.R.G. Townshend and R. Sohlberg, 2000: Global land cover classification at 1 km spatial resolution using a classification tree approach. Int. J. Remote Sensing, **21,** 1331-1364.

Kumar, S.V., C.D. Peters-Lidard, Y. Tian, P.R. Houser, J. Geiger, S. Olden, L. Lighty, J. L. Eastman, B. Doty, P. Dirmeyer, J. Adams, K. Mitchell, E.F. Wood and J. Sheffield, 2006: Land Information System - An interoperable framework for high resolution land surface modeling. *Environmental Modelling and Software*, **21,** 1402-1415.

Reichle, R. H., and R. Koster, 2004: Bias reduction in short records of satellite soil moisture, *Geophys. Res. Lett.,* L19501.